Geophys. J. R. astr. Soc. (1984) 78, 93–103

Induction in a thin sheet of variable conductance at the surface of a stratified earth – I. Two-dimensional theory

D. McA. McKirdy* and J. T. Weaver *Department of Physics, University of Victoria, PO Box 1700, Victoria, British Columbia V8W 2Y2, Canada*

Received 1983 October 10

Summary. An existing 2-D integral equation method for modelling electromagnetic induction in a thin sheet at the surface of a uniform half-space can be generalized to deal with a layered half-space by the inclusion of an extra term in the integral equation. The results obtained are shown to be in excellent agreement with finite difference solutions to the same modelling problem.

1 Introduction

The idea that thin conductivity anomalies near the surface of the Earth could be modelled by an infinitesimally thin sheet of variable conductance is attributed to Price (1949) and has subsequently been employed by many authors to study anomalous geomagnetic variations, particularly the coast effect.

Schmucker (1971) devised an algorithm employing convolution integrals to solve the problem of induction in a 2-D thin sheet overlying a layered substratum for the case of *E*-polarization and presented an inversion scheme for obtaining the anomalous conductance, subject to the restriction that the normal geoelectric structure was known. Green & Weaver (1978, hereafter referred to as G–W), solved the forward problem of induction in a thin sheet over a uniform half-space for both *E*- and *B*-polarizations and demonstrated how the kernels of the convolution integrals could be expressed in terms of modified Bessel functions.

Comparisons of the numerical solutions of G–W for the particular model of two half-sheets with the corresponding exact analytic solutions for both the *B*-polarization mode (Dawson & Weaver 1979a) and the *E*-polarization mode (Raval, Weaver & Dawson 1981; Dawson 1983) have shown that the numerical results are remarkably accurate especially in view of the fact that this particular model contains a jump discontinuity at the origin, which might be expected to pose problems for a numerical treatment.

In view of such excellent agreement with known analytic solutions it is believed that the method of G–W can be used to solve more complicated problems with some confidence. However, one limitation of the method, as originally published, was that the conducting half-space underlying the surface sheet was assumed to be uniform, rather than stratified. The purpose of this note is to show how the method can be extended by the simple inclus-

* Present address: Institute of Earth and Planetary Physics, University of Alberta, Edmonton, Alberta T6G 2J1, Canada.

sion of an extra term in the integral equation, to include a layered half-space beneath the sheet.

Three-dimensional models have been presented by Vasseur & Weidelt (1977) and Dawson & Weaver (1979b) but each method was subject to certain restrictions: the former could only deal with an anomalous zone of conductance surrounded by a uniform thin sheet, while the latter could model conductivity variations which reduced to a 2-D form at the edges of the model, but only over a uniform half-space. This paper is a precursor to a later paper showing how layers can be included in the 3-D algorithm of Dawson & Weaver. The *B*-polarization problem, not studied by Schmucker, is of particular interest when a generalized thin sheet, consisting of thin conducting and resistive layers, as devised by Ranganayaki & Madden (1980), is used. The existing 2- and 3-D algorithms can easily be modified to include this special kind of layering, which will also be demonstrated in a subsequent paper.

2 The model and basic equations

As in G–W we consider a 2-D earth model which has no variations in the x-direction and the external inducing field is assumed to be uniform and horizontal. The conducting part of the earth consists of an infinitesimally thin sheet of laterally varying conductance $\tau(y)$ overlying an N-layered half-space in which the nth layer, of conductivity σ_n, lies between the depths h_{n-1} and h_n, as shown in Fig. 1. For completeness we define h_0 to be zero and h_N to be infinity.

Two-dimensional induction problems can be expressed in terms of the *E*- or *B*-polarization modes when the direction of the inducing magnetic field is either perpendicular or parallel to the strike of a conductivity contrast. In the former case the electromagnetic field is $\mathbf{E} = (U, 0, 0)$ and $\mathbf{B} = (0, Y, Z)$, while in the case of *B*-polarization we have $\mathbf{E} = (0, V, W)$ and $\mathbf{B} = (X, 0, 0)$. All field components are independent of the variable x. A time-dependence

Following Dawson & Weaver (1979b), we find it convenient to deal in dimensionless variables. Distances are measured in terms of the skin depth $\delta = (2/\mu_0 \omega \sigma_0)^{1/2}$ where σ_0 is some representative conductivity which we shall eventually take to be the conductivity of the first layer. The magnetic field is measured in units of Y_0 (or X_0), the total field in the air at $y = \pm\infty$, and conductivities are all scaled by a factor $1/\sigma_0$. Consequently electric fields are measured in units of $\omega\delta Y_0$ (or $\omega\delta X_0$) and the units of conductance are $\delta\sigma_0$. (Note that the electric fields in G–W were plotted in units of $\omega\delta Y_0/2$ or $\omega\delta X_0/2$; the dimensionless fields introduced in this paper agree with the definitions of Dawson & Weaver (1979b) and calculated fields will be half the magnitude of the same fields calculated according to the practice of G–W.)

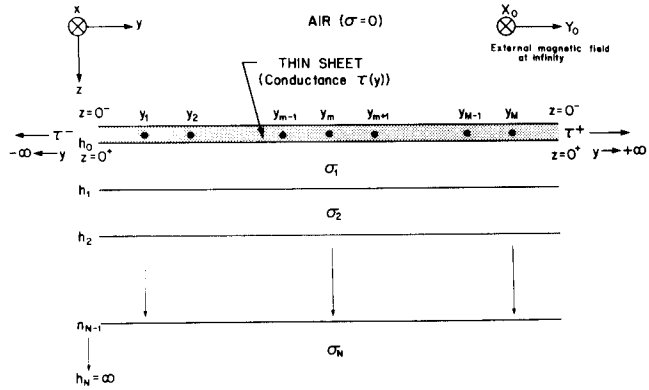

Figure 1. The mathematical model showing the layered structure and the numerical grid.

When the quasi-static approximation is used Maxwell's equations in dimensionless units are:

$$\nabla \times \mathbf{E} = -i\mathbf{B}, \qquad \nabla \times \mathbf{B} = 2\sigma\mathbf{E} \tag{2.1}$$

which in two dimensions reduce to two decoupled sets:

$$\begin{aligned} &\partial U/\partial y = iZ, && \partial V/\partial z - \partial W/\partial y = iX \\ &\partial U/\partial z = -iY, && \partial X/\partial z = 2\sigma V \\ &\partial Z/\partial y - \partial Y/\partial z = 2\sigma U, && \partial X/\partial y = -2\sigma W \end{aligned} \tag{2.2}$$

where each field component (F) obeys:

$$\partial^2 F/\partial y^2 + \partial^2 F/\partial z^2 = 2i\sigma F. \tag{2.3}$$

The thin sheet boundary conditions (G–W, equation 2.4) become

$$Y(y, 0+) - Y(y, 0-) = -2\tau(y)\,U(y, 0) \tag{2.4a}$$

$$X(y, 0+) - X(y, 0-) = 2\tau(y)\,V(y, 0). \tag{2.4b}$$

These two equations can be solved by using the appropriate Maxwell's equations to express the horizontal magnetic fields in terms of derivatives of the electric fields and in turn finding convolution integral formulae for these derivatives in terms of the horizontal electric field component U (or V). The resulting integral equation can be solved numerically.

3 Calculation of magnetic fields in terms of electric fields

In the E-polarization mode the calculation of $Y(y, 0-)$ is unaffected by the geoelectric structure of the half-space $z > 0$ and is given by G–W (equation 2.9) as

$$Y(y, 0-) = 1 - \frac{i}{\pi}\int_{-\infty}^{\infty} \frac{U(s, 0) - U(y, 0)}{(y - s)^2}\,ds. \tag{3.1}$$

The situation is even simpler in the B-polarization mode, where the magnetic field outside the conductor is uniform so that $X(y, 0-) = 1$, in dimensionless units. Therefore it is only necessary to find convolution integral formulae for $Y(y, 0+)$ and $X(y, 0+)$ in order to apply the boundary conditions (2.4a, b).

At this point it is convenient to proceed in Fourier space where the Fourier transform is defined by

$$\tilde{f}(\eta, z) = \frac{1}{\sqrt{2\pi}}\int_{-\infty}^{\infty} f(y, z)\exp(i\eta y)\,dy \tag{3.2}$$

and (2.3) becomes

$$\tilde{f}_{zz}(\eta, z) = (\eta^2 + 2i\sigma_n)\,\tilde{f}(\eta, z) = \gamma_n^2 \tilde{f}(\eta, z) \tag{3.3}$$

where the subscript notation for partial differentiation has been used. On taking the Fourier transform, in the generalized function sense, of the second equation in (2.2) we obtain

$$\tilde{U}_z(\eta, z) = -i\tilde{Y}(\eta, z), \tag{3.4}$$

and we can express $\tilde{U}_z$ in terms of $\tilde{U}$ by using the toroidal transfer function $\tilde{C}_T$ of Vasseur & Weidelt (1977), where

$$\tilde{C}_T(\eta) = -\tilde{U}(\eta, 0)/\tilde{U}_z(\eta, 0+). \tag{3.5}$$

The function $\tilde{C}_T(\eta)$ can be calculated as $\tilde{C}_1$ in the recursion relation (Schmucker 1971)

$$\tilde{C}_N = \gamma_N^{-1} \tag{3.6}$$

$$\tilde{C}_n = [\tilde{C}_{n+1}\beta_n + \tanh(\gamma_n d_n)/\gamma_n]/[1 + \beta_n\gamma_n\tilde{C}_{n+1}\tanh(\gamma_n d_n)], \tag{3.7}$$

($n = N-1, \ldots, 2, 1$), where $d_n \equiv h_n - h_{n-1}$ is the thickness of the nth layer measured in skin depths, and where for the toroidal mode under consideration $\beta_n = 1$. Actually we are interested in the reciprocal of the transfer function which can be written as

$$1/\tilde{C}_T(\eta) = \gamma_1 - \tilde{\phi}_T(\eta) \tag{3.8}$$

where by some algebraic manipulation it can be shown that

$$\tilde{\phi}_T(\eta) = -\gamma_1[1 - \tanh(\gamma_1 d_1)]\,(1 \quad \gamma_1\tilde{C}_2)/[\tanh(\gamma_1 d_1) + \gamma_1\tilde{C}_2]. \tag{3.9}$$

In the form (3.8) the reciprocal of the toroidal transfer function consists of a half-space contribution together with an additional term $\tilde{\phi}_T(\eta)$ which contains all the information about the layered structure. We now have from (3.5) and (3.8)

$$\tilde{U}_z(\eta, 0+) = \quad [\gamma_1 - \tilde{\phi}_T(\eta)]\tilde{U}(\eta, 0). \tag{3.10}$$

Strictly speaking a rigorous treatment of the Fourier inversion of this equation would require a lengthy discussion involving the theory of generalized functions, which would be inappropriate in a short note such as this. However, the required result can be obtained by inspection if we note that the first term on the right hand side of (3.10) corresponds to a uniform half-space beneath the thin sheet for which the required solution $U_z(y, 0+)$ can be quoted directly from G–W, while the second term involving $\tilde{\phi}_T$ can be Fourier inverted with the aid of the convolution theorem. Thus we find

$$-iY(y, 0+) = U_z(y, 0+) = -(1+i)\sqrt{\sigma_1}U(y, 0) + \frac{(1+i)}{\pi}\sqrt{\sigma_1}\int_{-\infty}^{\infty}\{U(s, 0) - U(y, 0)\}$$

$$\times \frac{K_1[(1+i)\sqrt{\sigma_1}\,|y-s|]}{|y-s|}\,ds + \frac{1}{\sqrt{2\pi}}\int_{-\infty}^{\infty}U(s, 0)\,\phi_T(y \quad s)\,ds \tag{3.11}$$

where K_1 is the modified Bessel function of the second kind and first order. The function ϕ_T must be calculated numerically. Since the definitions (3.9) and (3.7) clearly show $\tilde{\phi}_T(\eta)$ to be an even function, ϕ_T can be evaluated as the Fourier cosine transform

$$\phi_T(y) = \sqrt{\frac{2}{\pi}}\int_0^{\infty}\tilde{\phi}_T(\eta)\cos\eta y\,d\eta. \tag{3.12}$$

The situation is more complicated in the case of B-polarization when we have two terms to treat in the equation $iX = V_z - W_y$. In this mode the magnetic field and its vertical derivative are related by the poloidal transfer function

$$\tilde{C}_P(\eta) = -\tilde{X}(\eta, 0+)/\tilde{X}_z(\eta, 0+). \tag{3.13}$$

Now Maxwell's equations show that in a uniform medium

$$\tilde{V}_z(\eta, z)/\tilde{V}(\eta, z) = \tilde{X}_{zz}(\eta, z)/\tilde{X}_z(\eta, z), \tag{3.14}$$

and this applies, in particular, in the top layer below the thin sheet, where using (3.3) and (3.13) we can now write

$$\tilde{V}_z(\eta, 0+) = -\gamma_1^2 \tilde{C}_P(\eta)\, \tilde{V}(\eta, 0). \tag{3.15}$$

Here $\tilde{C}_P(\eta)$ can be calculated iteratively, as in (3.7), except that $\beta_n = \sigma_{n+1}/\sigma_n$ for this, the poloidal mode. We obtain after some algebraic manipulation

$$\tilde{C}_P(\eta) = 1/\gamma_1 + \tilde{\phi}_P(\eta)/2i\sigma_1 \tag{3.16}$$

where

$$\tilde{\phi}_P(\eta) = 2i\sigma_1[1 - \tanh(\gamma_1 d_1)](\sigma_2\gamma_1\tilde{C}_2 - \sigma_1)/\gamma_1[\sigma_1 + \sigma_2\gamma_1\tilde{C}_2 \tanh(\gamma_1 d_1)]. \tag{3.17}$$

Thus (3.15) becomes

$$\tilde{V}_z(\eta, 0+) = -(\gamma_1 + \gamma_1^2\phi_P(\eta)/2i\sigma_1)\tilde{V}(\eta, 0). \tag{3.18}$$

It remains to find an expression which links $\tilde{W}_y$ to $\tilde{V}$. The operator $\partial/\partial y$ transforms to $-i\eta$ in Fourier space and we obtain from Maxwell's equations and (3.13),

$$\tilde{W}(\eta, 0+) = (i\eta/2\sigma_1)[\tilde{X}(\eta, 0)/\tilde{X}_z(\eta, 0+)]\, \tilde{X}_z(\eta, 0+) = -i\eta\tilde{C}_P(\eta)\, \tilde{V}(\eta, 0). \tag{3.19}$$

If we multiply each side of (3.19) by $-i\eta$, substitute for $\tilde{C}_P$ from (3.16), and subtract from (3.18) we find

$$\tilde{V}_z(\eta, 0+) + i\eta\tilde{W}(\eta, 0+) = -[2i\sigma_1/\gamma_1 + \tilde{\phi}_P(\eta)]\, \tilde{V}(\eta, 0). \tag{3.20}$$

The inverse Fourier transform yields the desired result

$$iX(y, 0+) = V_z(y, 0+) - W_y(y, 0+)$$
$$= -\frac{2i\sigma_1}{\pi}\int_{-\infty}^{\infty} V(s, 0)K_0[(1+i)\sqrt{\sigma_1}|y-s|]\,ds - \frac{1}{\sqrt{2\pi}}\int_{-\infty}^{\infty} V(s, 0)\phi_P(y-s)ds. \tag{3.21}$$

Here the first integral is the corresponding one for the half-space (G–W, equation 3.20). The function ϕ_P can also be calculated as a Fourier cosine transform as defined in (3.12).

4 Construction of the integral equations

It is now a straightforward matter to substitute equations (3.1) and (3.11) into (2.4a) and (3.21) into (2.4b) to obtain the respective *E*- and *B*-polarization integral equations which can be solved numerically. If we also put $\sigma_1 = 1$ (see Section 2), then we obtain:

$$[1 + (1+i)\tau(y)]\, U(y, 0) = \frac{1+i}{2} + \frac{1}{\pi}\int_{-\infty}^{\infty} \{U(s, 0) - U(y, 0)\}\, G(y-s)\, ds$$
$$+ \frac{1-i}{2\sqrt{2\pi}}\int_{-\infty}^{\infty} U(s, 0)\phi_T(y-s)\, ds \tag{4.1}$$

where

$$G(s) = \frac{1-i}{2s^2} + \frac{K_1[|s|(1+i)]}{|s|} \tag{4.2}$$

as defined in G–W (equation 4.2). The B-polarization equation is:

$$\tau(y)\,V(y,0) = -\frac{1}{2} - \frac{1}{\pi}\int_{-\infty}^{\infty} V(s)\,K_0[(1+i)|y-s|]\,ds$$

$$+\frac{i}{2\sqrt{2\pi}}\int_{-\infty}^{\infty} V(s,0)\,\phi_P(y-s)\,ds. \tag{4.3}$$

In both cases the effect of layering is to introduce a second integral into the equation, the kernel of which is always well behaved and can be easily calculated numerically.

5 Calculation of other field components

Once the horizontal electric field $U(y,0)$ has been found it is simple to calculate $Y(y,0-)$, the horizontal magnetic field above the thin sheet, by using equation (3.1). The corresponding magnetic field just below the sheet is then given by:

$$Y(y,0+) = (1-i)\,U(y,0) - \frac{1-i}{\pi}\int_{-\infty}^{\infty} \{U(s,0) - U(y,0)\}\,\frac{K_1[(1+i)|y-s|]}{|y-s|}\,ds$$

$$+\frac{i}{\sqrt{2\pi}}\int_{-\infty}^{\infty} U(s,0)\,\phi_T(y-s)\,ds. \tag{5.1}$$

With B-polarization it is known that $X(y,0-) = 1$ and the magnetic field below the thin sheet can be found by using the thin sheet boundary condition, i.e.

$$X(y,0+) = 1 + 2\tau(y)\,V(y,0). \tag{5.2}$$

The simplest way to calculate the vertical fields $Z(y,0)$ and $W(y,0+)$ which arise in the E- and B-polarization problems respectively is to use finite difference approximations to the first and last Maxwell's equations (2.2). They can yield accurate values of Z or W since the fields U and X are always continuous even where there are lateral discontinuities in the conductance $\tau(y)$. However, an integral expression for W can be derived from (3.19) and a similar one can be found for Z. Equation (3.19) can be rewritten as

$$\tilde{W}(\eta,0+) = \tilde{C}_P(\eta)\,V_y(\eta,0) \tag{5.3}$$

and after substituting (3.16) we obtain

$$\tilde{W}(\eta,0+) = [1/\gamma_1 + \tilde{\phi}_P(\eta)/2i]\,\tilde{V}_y(\eta,0). \tag{5.4}$$

Inversion leads to

$$W(y,0+) = \frac{1}{\pi}\int_{-\infty}^{\infty} V_y(s,0)\,K_0[(1+i)|y-s|]\,ds$$

$$-\frac{i}{2\sqrt{2\pi}}\int_{-\infty}^{\infty} V_y(s,0)\,\phi_P(y-s)\,ds \tag{5.5}$$

and an integration by parts yields

$$W(y, 0+) = -\frac{1+i}{\pi} \int_{-\infty}^{\infty} \operatorname{sgn}(y-s) V(s, 0) K_1[(1+i)|y-s|]\, ds$$
$$-\frac{i}{2\sqrt{2\pi}} \int_{-\infty}^{\infty} V(s, 0)\, \phi'_{\mathrm{P}}(y-s)\, ds. \tag{5.6}$$

Here ϕ'_{P} is calculated numerically as the Fourier sine transform

$$\phi'_{\mathrm{P}}(y) = -\sqrt{\frac{2}{\pi}} \int_0^{\infty} \eta \tilde{\phi}_{\mathrm{P}}(\eta) \sin \eta y\, d\eta \tag{5.7}$$

which follows by differentiating ϕ_{P} expressed as a cosine Fourier transform (see 3.12). In E-polarization it can be deduced from the first of Maxwell's equations (2.2) that

$$\tilde{Z}(\eta, 0) = \tilde{C}_{\mathrm{T}}(\eta)\, \tilde{U}_y(\eta, 0). \tag{5.8}$$

This is analogous to (5.3) and a similar analysis gives the following expression for the vertical magnetic field

$$Z(y, 0) = -\frac{1+i}{\pi} \int_{-\infty}^{\infty} \operatorname{sgn}(y-s) Y(s, 0+) K_1[(1+i)|y-s|]\, ds$$
$$+\frac{1}{\sqrt{2\pi}} \int_{-\infty}^{\infty} Y(s, 0+)\, \phi'(y-s)\, ds \tag{5.9}$$

where

$$\phi'(y) = -\sqrt{\frac{2}{\pi}} \int_0^{\infty} \eta \tilde{\phi}_z(\eta) \sin \eta y\, d\eta \tag{5.10}$$

and

$$\tilde{\phi}_z(\eta) = [\tanh(\gamma_1 d_1) - 1](1 + \gamma_1 \tilde{C}_2)/\gamma_1 [1 + \gamma_1 \tilde{C}_2 \tanh(\gamma_1 d_1)]. \tag{5.11}$$

The $\tilde{C}_n$ are calculated iteratively as in equation (3.7) with $\beta_n = 1$.

6 Numerical considerations

It has been shown in Section 4 that the integral equations for a layered half-space consist of the equations derived by G–W with an extra integral as a correction term. The kernels of these correction terms are well behaved and non-singular so the new term can easily be incorporated into the existing numerical scheme.

As in G–W the variable conductance is assigned to the $M-1$ intervals between the M nodes y_m $(m = 1, \ldots, M)$ of the numerical grid. The conductance is assumed constant beyond the edges of the grid, i.e.

$$\tau(y) = \begin{cases} \tau_-\ (y < y_1), \\ \tau_+\ (y > y_M). \end{cases} \tag{6.1}$$

The integral equation is solved exactly as is G–W. Only the method of treating the additional integrals (those containing the information on the layered structure) will be described here.

Because the kernels in the additional integrals are so well-behaved, it is sufficient to assume that the field is constant in each cell. The second integral in equation (4.1) evaluated at y_μ can be written with the aid of (3.12) in the form

$$\sum_{m=0}^{M} \bar{U}_m \int_{y_m}^{y_{m+1}} \phi_T(y_\mu - s)\, ds$$

$$= \sum_{m=0}^{M} \bar{U}_m \sqrt{\frac{2}{\pi}} \int_{y_m}^{y_{m+1}} \int_0^\infty \tilde{\phi}_T(\eta) \cos\left[\eta(y_\mu - s)\right] d\eta ds, \tag{6.2}$$

where $\bar{U}_m (m = 0, 1, \ldots, M)$, is a suitable constant value for $U(y, 0)$ in the interval $[y_m, y_{m+1}]$, and where we have defined $y_0 = -\infty$ and $y_{M+1} = +\infty$. Interchanging the order of the integrations, integrating once and rearranging the summation we obtain

$$\int_{-\infty}^{\infty} U(s, 0)\, \phi_T(y - s)\, ds \approx \sqrt{\frac{2}{\pi}} \sum_{m=1}^{M} (\bar{U}_m - \bar{U}_{m-1}) \int_0^\infty \frac{\tilde{\phi}_T(\eta)}{\eta} \sin\left[\eta(y_\mu - y_m)\right] d\eta. \tag{6.3}$$

The first and last integrals in the summation have disappeared by virtue of the Riemann–Lebesgue lemma. For the calculation given in this paper we set

$$\bar{U}_m = \begin{cases} U(y_{m+1}, 0) & (0 \leqslant m \leqslant \mu - 1) \\ U(y_m, 0) & (\mu \leqslant m \leqslant M) \end{cases}$$

although other choices, such as the mean value of U in the inverval, are possible. In order to be able to evaluate each integral on the right hand side of (6.3) it is necessary to calculate the Fourier sine transform of $\tilde{\phi}_T(\eta)/\eta$ numerically. This was done by using a suitable FFT package, but to avoid any numerical problems near $\eta = 0$ it was found best to calculate the transform in (6.3) in the form

$$\int_0^\infty \tilde{\phi}_T(\eta) \sin \eta(y_\mu - y_m) d\eta = \frac{1}{2} \pi \tilde{\phi}_T(0) + \int_0^\infty \frac{\{\tilde{\phi}_T(\eta) - \tilde{\phi}_T(0)\}}{\eta} \sin\left[\eta(y_\mu - y_m)\right] d\eta. \tag{6.4}$$

All of the new correction terms can be treated similarly so that the only numerical calculations required are those to evaluate the inverse Fourier transforms.

Results

A purely synthetic model has been chosen consisting of two thin half-sheets, with a conductance contrast of 4 : 1, overlying a three layered earth, the details of which appear in Table 1 in both SI and dimensionless units. The period of the inducing field is 1000 s and the dimensionless conductances are $\tau_- = 4$ and $\tau_+ = 1$.

Table 1. Model parameters.

	SI units	Dimensionless units
σ_1	0.008 S m^{-1}	1
σ_2	0.002 S m^{-1}	0.25
σ_3	0.333 S m^{-1}	41.67
d_1	50 km	0.281
d_2	110 km	0.618

Traverse plots of the electromagnetic field components are shown in Figs 2–4 for the *E*- and *B*-polarization cases. The general shapes of these graphs match those of published analytic results when a uniform half-space was used to simulate the Earth (Dawson & Weaver 1979a and Dawson 1983). In *E*-polarization the electric field U is continuous, the magnetic

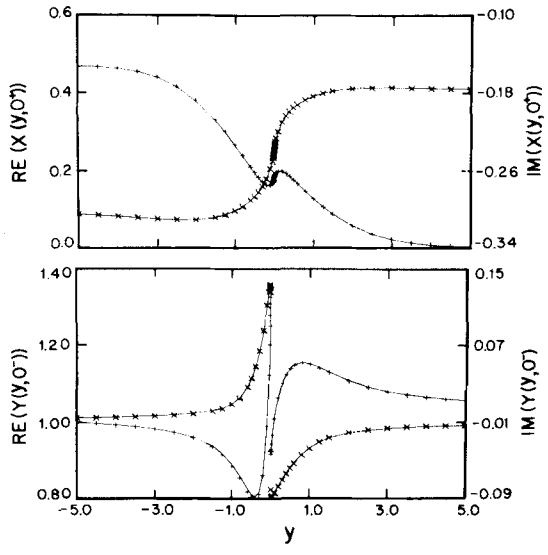

Figure 2. Plots of the dimensionless horizontal magnetic field components. The upper diagram shows the *B*-polarization field $X(y, 0+)$ at the lower surface of the thin sheet while the *E*-polarization field in the lower diagram, $Y(y, 0-)$, is calculated in air. Distances are measured in skin depths from the discontinuity in conductance at the origin. The solid lines show the results of the method presented in this paper and the crosses and plus signs show the real and imaginary parts of results obtained by the method of Brewitt-Taylor & Weaver respectively.

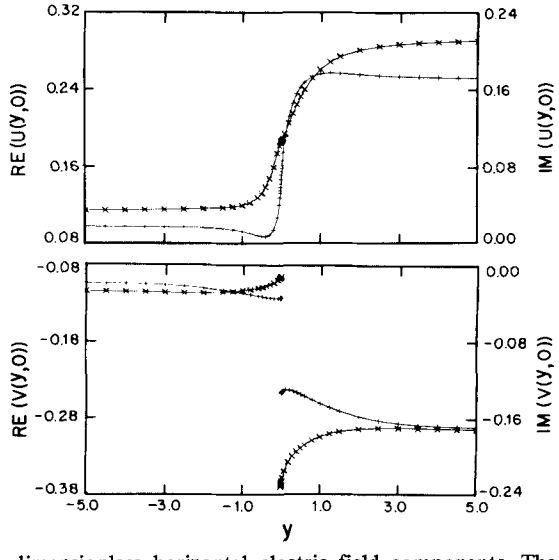

Figure 3. Plots of the dimensionless horizontal electric field components. The upper diagram shows $U(y, 0)$, the solution to *E*-polarization integral equation, while the lower diagram shows $V(y, 0)$, the *B*-polarization solution. The notation is as given in Fig. 2.

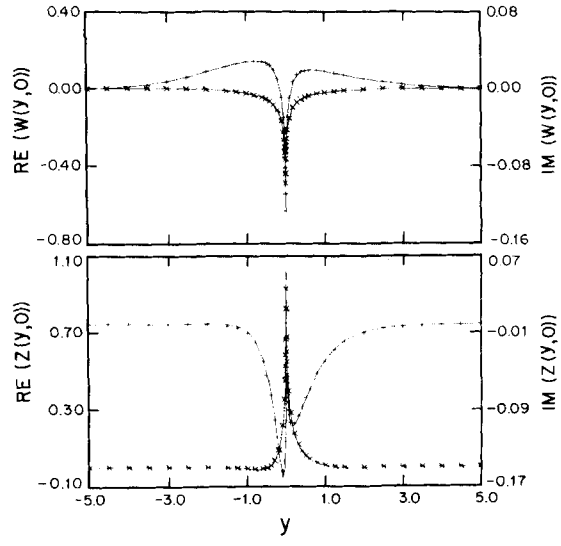

Figures 4. Plots of the dimensionless vertical field components. The upper diagram shows the electric field $W(y, 0+)$ present in the B-polarization problem while the lower diagram shows the magnetic field $Z(y, 0)$ which arises in the E-polarization case. The notation is as given in Fig. 2.

field Y is discontinuous and the vertical magnetic field Z is most pronounced in the region of the conductance discontinuity. With B-polarization the X field is continuous while the electric field V is discontinuous across the boundary and the vertical electric field W, indicating the vertical leakage into the substratum, is greatest near the conductance contrast. Actually the magnitude of the vertical current is greater on the more conducting side of the interface.

Nicoll & Weaver (1977) published an analytic solution for the B-polarization mode only in which two perfectly conducting and insultating thin half-sheets were located at the surface of a two-layered earth which had a perfectly conducting basement. These results did not appear in a tabulated form; therefore no attempt was made to compare their results with the method presented here but this does not seem too serious in view of the extreme conductivities used. Instead our results are compared with those from the finite difference algorithm of Brewitt-Taylor & Weaver (1976), which are denoted by crosses in Figs 2–4. The comparison is clearly favourable in all of the diagrams shown. The vertical field components Z and $W+$ in Fig. 4 have been calculated using the appropriate integral formulae.

Both E- and B-polarization results were obtained in less than 3 min on a 57×1 numerical grid using the method described in this paper, while the finite difference algorithm required 13 min to solve the E-polarization problem using a 56×50 grid and 5 min to obtain the solution to the B-polarization problem on a 59×38 grid. An IBM 4341 machine was used to perform all of the calculations.

The asymptotic boundary conditions for E-polarization presented in Weaver & Brewitt–Taylor (1978) and used by G–W have also been incorporated into the present scheme with little additional effort.

Conclusions

It has been demonstrated that it is not difficult to extend the 2-D theory of Green & Weaver (1978) to permit the use of a layered earth when modelling thin surface conductivity

anomalies with a thin sheet. The work treats both electromagnetic modes, and the solutions obtained agree very closely with those resulting from the application of finite difference methods with an appreciable saving in computer time.

Although the results obtained from these 2-D studies have limited application to real geophysical structures they do serve as a useful check on the accuracy of results obtained from a generalized form of the algorithm of Dawson & Weaver (1979b) which incorporates a layered substratum and this will be demonstrated in a further paper.

Acknowledgments

Dr Trevor W. Dawson is thanked for many helpful discussions in connection with this work. The authors gratefully acknowledge the support of the Natural Sciences and Engineering Research Council of Canada.

References

Brewitt-Taylor, C. R. & Weaver, J. T., 1976. On the finite difference solution of two-dimensional induction problems. *Geophys. J. R. astr. Soc.*, **47**, 375–396.

Dawson, T. W., 1983. *E*-polarization induction in two thin half-sheets, *Geophys. J. R. astr. Soc.*, **73**, 83–107.

Dawson, T. W. & Weaver, J. T., 1979a. *H*-polarization induction in two thin half-sheets, *Geophys. J. R. astr. Soc.*, **56**, 419–438.

Dawson, T. W. & Weaver, J. T., 1979b. Three-dimensional electromagnetic induction in a non-uniform thin sheet at the surface of a uniformly conducting earth, *Geophys. J. R. astr. Soc.*, **59**, 445–462.

Green, V. R. & Weaver, J. T., 1978. Two-dimensional induction in a thin sheet of variable integrated conductivity at the surface of a uniform conducting earth, *Geophys. J. R. astr. Soc.*, **55**, 721–736.

Nicoll, M. A. & Weaver, J. T., 1977. *H*-polarization induction over an ocean edge coupled to the mantle by a conducting crust, *Geophys. J. R. astr. Soc.*, **49**, 427–442.

Price, A. T., 1949. The induction of electric currents in non-uniform thin sheets and shells, *Q. Jl Mech. appl. Math.*, **2**, 283–310.

Ranganayaki, R. P. & Madden, T. R., 1980. Generalized thin sheet analysis in magnetotellurics: an extension of Price's analysis, *Geophys. J. R. astr. Soc.*, **60**, 445–457.

Raval, U., Weaver, J. T. & Dawson, T. W., 1981. The coast effect reexamined, *Geophys. J. R. astr. Soc.*, **67**, 115–123.

Schmucker, U., 1971. Interpretation of induction anomalies above non-uniform surface layers, *Geophysics*, **36**, 156–165.

Vasseur, G. & Weidelt, P., 1977. Bimodal electromagnetic induction in non-uniform thin sheets with an application to the northern Pyrenean induction anomaly, *Geophys. J. R. astr. Soc.*, **51**, 669–690.

Weaver, J. T. & Brewitt-Taylor, C. R., 1978. Improved boundary conditions for the numerical solution of *E*-polarization problems in geomagnetic induction, *Geophys. J. R. astr. Soc.*, **54**, 309–317.